

# Bioinspired Simulation of Knotting Hagfish

Yura Hwang<sup>1\*</sup>, Theodore A. Uyeno<sup>2†</sup>, and Shinjiro Sueda<sup>1‡</sup>

<sup>1</sup> Department of Computer Science & Engineering, Texas A&M University

<sup>2</sup> Department of Biology, Valdosta State University

**Abstract.** Hagfish are capable of not only forming knots, but also sliding them along the length of their bodies. This remarkable behavior is used by the animal for a wide variety of purposes, such as feeding and manipulation. Clearly of interest to biologists, this knotting behavior is also relevant to other fields, such as bioinspired soft robotics. However, this knot-sliding behavior has been challenging to model and has not been simulated on a computer. In this paper, we present the first physics-based simulation of the knot-sliding behavior of hagfish. We show that a contact-based inverse dynamics approach, motivated by the biological concept called *positive thigmotaxis*, works very well for this challenging control problem.

**Keywords:** Simulation · biology · physics-based · knots

## 1 Introduction

Hagfish are incredibly flexible animals. Their flexibility is best demonstrated by their ability to tie their long skinny bodies into knots and effectively manipulate those knots for many purposes: they wipe their bodies clean by passing knots from one end to the other [1]; they can use knots to extricate themselves from burrows and holes [31,40]; and knots are used to generate leverage in order to tear off chunks of food [11]. This last function of knotting is interesting because hagfish evolved prior to the evolution of vertebrate jaws, and yet they are able to remove considerable morsels while scavenging carrion, such as the decaying carcasses of whales. This is achieved by first embedding the teeth of an eversible toothplate into the food item, forming a knot at the tail, and then *sliding this knot* anteriorly until a loop of the knot passes over the hagfish’s head. This loop is pressed up against the food item and is used as powerful leverage to tear out the morsel [12,37].

While there are other vertebrates that are capable of knotting, namely sea-snakes (e.g. [27]) and moray eels (e.g. [24]), hagfish seem to be the most ready to employ knotting behaviors and are capable of tying the greatest variety of knots. This may be because they possess extensive adaptations for creating and manipulating body knots. First, their bodies are flexible and extremely elongate;

---

\*chizuru97@tamu.edu

†tauyeno@valdosta.edu

‡sueda@tamu.edu

their lengths are typically over twenty times that of their widths [16]. Second, hagfish have no fins or other projections that extend from their rope-like bodies. Third, their skins lack the outer layer that produce rough scales, resulting in a smooth skin with low friction [3]. Fourth, their skins are extremely baggy and loosely connected to the musculature of the body wall, which precludes the tough skin from binding during knotting maneuvers [10]. Fifth, the body does not have a spinal column, or any bones at all, to stiffen the body; instead a flexible, cartilaginous rod (the notochord) that extends down the length of the inextensible body accounts for most of the body stiffness [22].

The extreme flexibility represents a neural control problem that is poorly understood, because controlling such flexibility may theoretically require an enormous amount of neural input [38]. Such models and organisms are described as “hyper-redundant” [36]. As a result, researchers have not only been unable to characterize how hagfish control their bodies during this *knot formation and manipulation* process, but they also have struggled to develop a computer simulation of knotting that appears realistic or biologically informative.

The key to developing a realistic simulation of a knotting hagfish rests on a behavioral characteristic known as “positive thigmotaxis,” which describes an animal’s drive to be in direct physical contact with solid objects in its local environment. Our own observations of hagfish in aquaria confirm that they seem to prefer to be pressed up against the edges or touching others, rather than be alone or in the center of the aquarium. This positive thigmotaxis may stem from their real world behaviors of living in shallow burrows or crevices in the dark zones of the ocean or packing tightly into cavities of whale carcasses [23,40]. In reviewing high speed videos of knotting hagfishes, Haney noticed that the tail exhibits positive thigmotaxis during all stages of knot formation and manipulation [16]. The type of knots that hagfish make depends on the number of crossovers that the tail forms. Interestingly, mathematicians who study knots also categorize them by the number and organization of crossovers [2]. The key feature that we have noticed is that as the hagfish slide a given knot anteriorly or posteriorly along the body, the constituent crossovers do not change in relation to each other. Our contact-based inverse dynamics approach is motivated by this observation.

In this paper, we present a novel graphics testbed for simulating a knotting hagfish. Our main contribution is that our work is the first demonstration of the knot forming *and sliding* behavior. We use reduced coordinate rigid body dynamics to model the hagfish with parameters taken from real-world measurements (§3.1). We then apply a contact-based inverse dynamics controller based on positive thigmotaxis that produces a realistic and bioinspired knot sliding movement of the hagfish (§3.2).

## 2 Related Work

**Knotting of Hagfish** The knotting behavior of hagfish was first documented by Adams [1], who observed that *Myxine glutinosa*, or Atlantic hagfish, formed a knot to clean off slime from its body. He also observed that the movement can

be reversed—the knot can slide toward the head or the tail. Ever since, most works focused on specific functional uses of knotting behavior, which hagfishes exploit for their survival. These include wriggling out of burrows and leveraging retractile force against the surface to tear out morsels of food [11,12,37,40]. There are also some works that looked into the biomechanisms involved in the knotting process. Haney [16] focused on different kinds of knots that hagfish are capable of formulating, and Evans et al. [14] analytically examined the body flexibility of hagfish based on biometric data. In this paper, we use their observations and measurements to simulate the knot forming and sliding.

**Simulation of (Sliding) Rods and Cables** There exist many approaches for the dynamic simulation of rods and cables that could be used for hagfish simulation [25,7,6,32,13]. In our work, we use rigid body dynamics, which has been an active research area for decades [15]. In computer graphics, the classical work by Baraff presented an efficient method for computing contact and friction forces acting on rigid bodies [4]. In the past decade, a number of works have studied how to combine rigid and deformable bodies [29,19,17,21,39]. In our work, we use only the rigid degrees of freedom, and deform the skin mesh using splines, which is used for contact with the environment and itself. Our dynamics simulator uses the REDMAX formulation by Wang et al. [39]. However, our *positive thigmotaxis* approach can be used by any simulator as long as they support inverse dynamics with contact. Frictional contact [18] is out of scope of our work, since hagfish possess smooth, water-lubricated skin that effectively eliminates friction. Finally, some researchers have specifically studied knot tying [26,9], but their systems cannot be used for knot *sliding*, which is the focus of our work.

**Neural Control** The extreme flexibility exhibited by hagfish represents a neural control problem that is poorly understood by biologists, although several studies have begun to investigate several examples. For example, Sumbre et al. presented a motor primitive of an octopus reaching its arm toward a 3D target point [34]. Motivated by biology, roboticists have worked on designing and controlling soft robots [30,36,28]. In biomechanics, the standard approach for computing the control signal of skeletal animals has been to use computed muscle control [35], and in computer graphics, similar methods have been proposed [33,20]. However, these methods do not consider knot forming or sliding, which is the primary focus of our work.

### 3 Methods

In this section, we first describe our simulation framework (§3.1), followed by our control strategy for knot forming and sliding (§3.2).

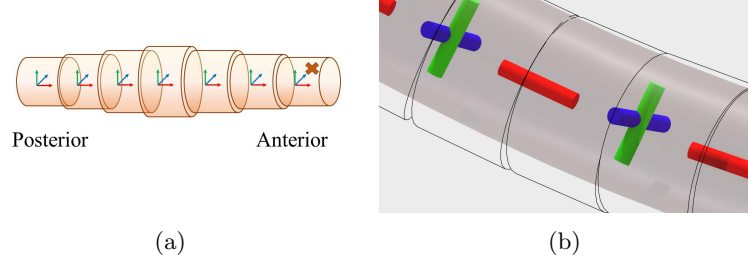


Fig. 1: The simplified representation of our hagfish model (a), and a zoomed view of hagfish anatomy (b), where it consists of revolute joints and universal joints.

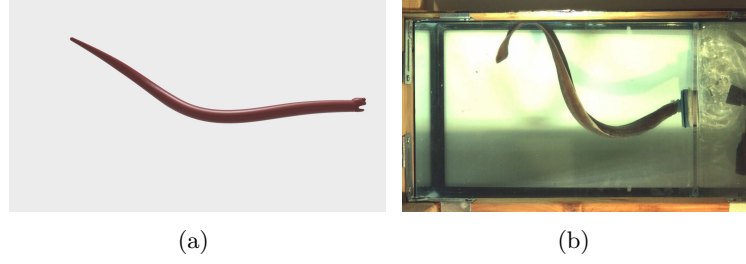


Fig. 2: We fixed our hagfish’s head to the wall (a), to match the video (b).

### 3.1 Simulator

We use 100 rigid bodies and joints, aligned along the X-axis. Although hagfish are flexible, using rigid bodies is a reasonable approximation, since their cartilaginous spine is flexible and inextensible. These rigid bodies are connected with X-revolute joints and YZ-universal joints in an alternating fashion. This allows us to apply our biometric data on twisting limits on revolute joints and bending limits on universal joints (Figure 1), which is difficult to do with spherical joints. These and other parameters of the simulation are obtained from real-world measurements, and are listed in §4.

We use forward Euler integration to advance the rigid bodies in time. When there are no constraints, we solve the following linear system:

$$M\dot{q} = M\dot{q}_0 + hf, \quad (1)$$

where  $M$  is the mass matrix,  $\dot{q}$  is the new velocity vector we are solving for,  $\dot{q}_0$  is the velocity from the last time step,  $h$  is the fixed time step, and  $f$  is the force vector, which includes all internal, external, and Coriolis forces. Once the velocities are computed, we update the positions as

$$q = q_0 + h\dot{q}. \quad (2)$$

During the course of a simulation, we encounter various types of constraints. Bilateral constraints are used to fix the head to the wall, to match the video.

(See Figure 2; the head was gently held by a rubber collar in order to facilitate imaging.) This constraint may be released during the simulation to allow the head to release from the wall. Unilateral constraints are used for joint limits, contact with the wall, and self-contact. If there exists only bilateral constraints, we solve the problem using Karush-Kuhn-Tucker (KKT) system [8]:

$$\begin{pmatrix} M & G^\top \\ G & 0 \end{pmatrix} \begin{pmatrix} \dot{q} \\ \lambda \end{pmatrix} = \begin{pmatrix} M\dot{q}_0 + hf \\ 0 \end{pmatrix}, \quad (3)$$

where  $G$  is the Jacobian of the constraints, and  $\lambda$  is the vector of Langrange multipliers. If there exist both bilateral and unilateral constraints, we solve the following quadratic program:

$$\begin{aligned} & \underset{\dot{q}}{\text{minimize}} && \frac{1}{2} \dot{q}^\top M \dot{q} - \dot{q}^\top (M\dot{q}_0 + hf) \\ & \text{subject to} && G\dot{q} = 0, \quad C\dot{q} \geq 0, \end{aligned} \quad (4)$$

where  $G$  and  $C$  are the Jacobians of bilateral and unilateral constraints, respectively. Since the constraints are enforced at the velocity level, the system may drift away from the constraint manifold. To counter this, we stabilize the positions when necessary [5].

**Contact Handling** Collision detection and contact handling are important aspects of this work, given that our work is inspired by positive thigmotaxis. Collisions can come from either self collisions during knotting, or from the body hitting the head plate of the tank.

For collision detection, we use a Catmull-Rom spline curve passing through the center of each rigid body, which represents the cartilaginous spine of the hagfish (Figure 3a). We first find two colliding rigid bodies using bounding spheres around each rigid body. Once colliding spheres are detected, we find the closest points between these two segments of the spline curve using Newton’s method, by looking for the zero of the following function:

$$f(t_i, t_j) = \begin{pmatrix} x'(t_i)^\top (x(t_j) - x(t_i)) \\ x'(t_j)^\top (x(t_j) - x(t_i)) \end{pmatrix}, \quad (5)$$

where  $t_i$  and  $t_j$  are the parameters of the spline curve;  $x(t_i)$  and  $x(t_j)$  are positions along the curve; and  $x'(t_i)$  and  $x'(t_j)$  are derivatives, respectively. Once these points are computed, we check if the distance between them are shorter than the sum of the radii at these two points. If so, the contact constraint is added to the unilateral constraint matrix,  $C$ , in Eq. 4.

### 3.2 Controller

The controller consists of two independent steps: forward dynamics and inverse dynamics, for knot forming and knot sliding, respectively.

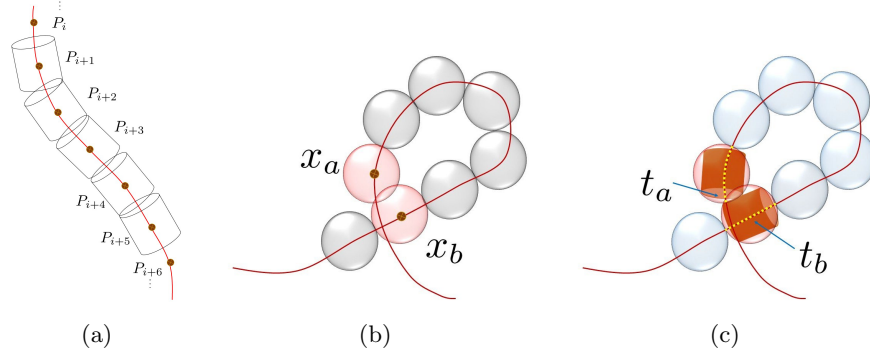


Fig. 3: Illustration of overall collision detection process. (a) We represent our hagfish using spline curve. (b) We find two colliding rigid bodies using bounding spheres. (c) The exact colliding points of collided rigid bodies are computed using Newton’s method.



Fig. 4: Simulation of knot formulation. We closely follow each kinematic steps of hagfish behavior: (a) body crossover, (b) tail wrap, and (c) tail insertion. The labeled tangents in (c) are for the thigmotaxis constraints used in knot sliding.

**Knot Forming** To form the knot, we use forward dynamics with scripted forces. In order to formulate a knot, we follow the kinematic steps of body crossover, tail wrap, and tail insertion. For each time step, we apply a sequence of scripted forces on the terminal body of the hagfish to manipulate the behavior, as shown in Figure 5. Although torques can be applied as well, we found that linear forces were enough to produce the initial knot. Forming a knot using a sequence of scripted forces is time consuming, but fairly easy to achieve. On the other hand, the same method cannot easily be used for sliding the knot along the body, which we discuss next.

**Knot Sliding** There is no intuitive way to apply forces or torques to make the knot slide. We overcome this difficulty by using a novel *contact-based inverse*

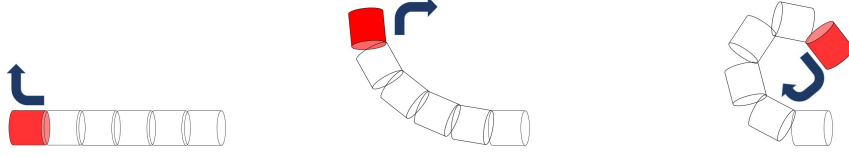


Fig. 5: Illustration of knot manipulation. We manipulate the terminal body to form a knot.

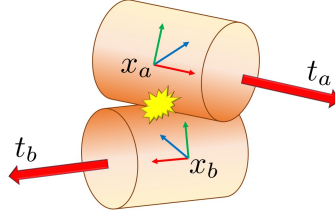


Fig. 6: Illustration of our contact-based inverse dynamics.

*dynamics* approach based on positive thigmotaxis, which is the main technical contribution of this paper.

Once we detect self collisions due to the tail forming the knot, we switch the controller from forward dynamics to inverse dynamics. In inverse dynamics, we compute the forces and torques given a specified motion. This can be cast as a constraint to be applied to the motion [39]. Specifically, for self-collision points, we require that the projection of the relative velocity between the two contacting points onto the tangent direction be greater than some value. Mathematically, this can be written as:

$$\begin{aligned} t_a^\top (\dot{x}_a - \dot{x}_b) &\geq v_a \\ t_b^\top (\dot{x}_b - \dot{x}_a) &\geq v_b, \end{aligned} \quad (6)$$

where  $t_a$  and  $t_b$  are the unit tangent vectors of the colliding rigid bodies,  $\dot{x}_a$  and  $\dot{x}_b$  are the world velocities of the colliding points, and  $v_a$  and  $v_b$  are scalar parameters to control the sliding motion in tangential directions. Figure 6 illustrates these quantities. All of these quantities can be computed as functions of the current generalized positions and velocities,  $q$  and  $\dot{q}$  [39]. These constraints are added to the unilateral constraint matrix in Eq. 4.

In general, there are many self-collisions during a knotting process. We do not use all of them, as this could lead to an overly constrained problem. Instead, we sort the collisions by the parametric distance from the head, and apply the thigmotaxis constraint to only the first and last collisions. These two constraints with their respective tangents ( $t_a$  and  $t_b$ ) are shown in Fig. 4c. We can manipulate the knot by changing the  $v_a$  and  $v_b$  parameters of these two constraints. We use two substeps. First, we tighten the knot by using different values between the two

constraints, which shortens the portion of the hagfish tied into the knot. Once the knot is sufficiently tight, we set the parameters to be the same for both constraints, which forces the hagfish to slide the knot along its body toward the head. The parameters used in our simulation are listed in Table 1.

The forces computed by the inverse dynamics solver can be calculated with the Lagrange multipliers of the quadratic program in Eq. 4. Let  $\lambda$  be the vector of Lagrange multipliers corresponding to the inequality constraints. Let us also divide the unilateral constraint Jacobian and the Lagrange multiplier into three parts corresponding to the joint limits, collisions, and thigmotaxis:

$$C = \begin{pmatrix} C_{\text{limits}} \\ C_{\text{collision}} \\ C_{\text{thigmo}} \end{pmatrix}, \quad \lambda = \begin{pmatrix} \lambda_{\text{limits}} \\ \lambda_{\text{collision}} \\ \lambda_{\text{thigmo}} \end{pmatrix}. \quad (7)$$

Then the inverse dynamics force from positive thigmotaxis can be computed as:

$$f_{\text{thigmo}} = \frac{1}{h} C_{\text{thigmo}}^\top \lambda_{\text{thigmo}}. \quad (8)$$

## 4 Results

We implemented our simulation using C++, and ran our experiments on a consumer desktop with an Intel Core i7-7700 CPU 3.6 Ghz and 16 GB of RAM. We used Eigen for linear algebra computations and Mosek for quadratic programs.

Table 1 lists the biometric data and parameters for inverse dynamics that were used in our simulation. Figure 7 shows a visual comparison between our simulation and real hagfish restrained in the tank. Our method is able to simulate the sliding movement of the knot realistically. The first three pairs of images show the real and virtual animal form the knot with the tail. During this stage, the

Table 1: Biometric data and inverse dynamics parameters. The specimen was measured at 20% increments in length; the four values for circumference and bending limit are for 20%, 40%, 60%, and 80%, respectively, from head to tail. Intermediate values are linearly interpolated. The twisting limit was measured for the whole body, and was divided by the number of rigid bodies.

Data	Values	Units
Length	42.4	cm
Mass	80	g
Circumference	5.6, 5.5, 5.6, 4.3	cm
Bending limit	21, 75, 45, 51	deg
Twisting limit	48	deg
$v_a, v_b$ (tightening, head)	0.0, 0.0	cm/s
$v_a, v_b$ (tightening, tail)	0.5, 2.0	cm/s
$v_a, v_b$ (sliding, head)	2.0, 2.0	cm/s
$v_a, v_b$ (sliding, tail)	2.0, 2.0	cm/s

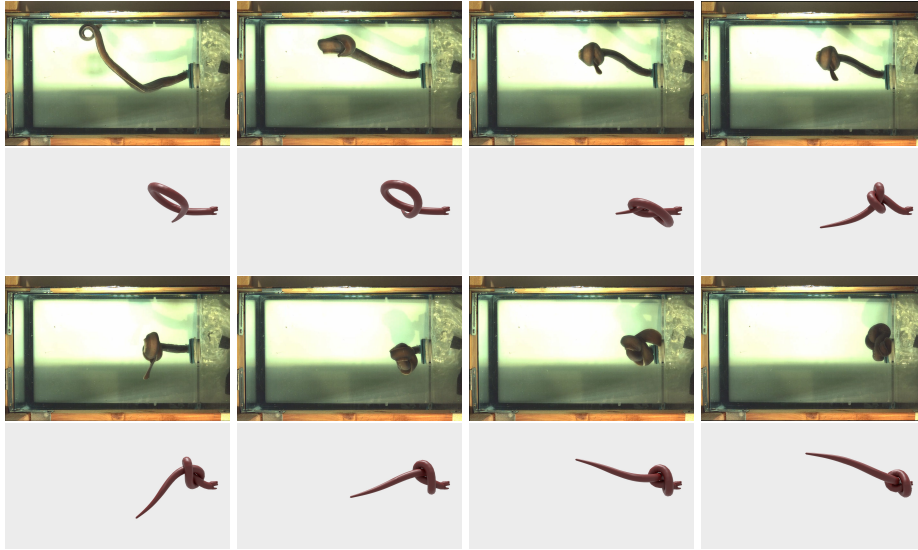


Fig. 7: Our result of knotting hagfish with *positive thigmotaxis*. The above row shows the actual video of hagfish restrained in a tank, and below shows our simulation.

virtual hagfish is driven using a manually scripted forward dynamics controller. The next five pairs of images show the animal sliding the knot toward the head. During this stage, the virtual hagfish is driven using our contact-based inverse dynamics controller.

Figure 8 shows the plot of force with time and joints during the knot sliding phase. The three subfigures are the X, Y, and Z torques, respectively. The vertical axis shows the force computed by the inverse dynamics controller. The two horizontal axes show the time in seconds and the joint number (head = 0, tail = 50).<sup>‡</sup> As is typically the case, the forces produced by inverse dynamics is noisy. However, we can see some interesting patterns. First, as the knot moves toward the head over time, the forces acting on joints closer to the tail become zero, as expected. This is because once the knot has passed over a joint, that joint no longer needs to be controlled to move the knot. In the graph, this can be seen as a flat triangular region to the right of each graph. Second, more force is required when the knot approaches the head. This is because the head is attached to the plate, and so manipulating the knot requires moving the whole length of the animal from head to tail. Third, even though the forces rapidly change along the temporal dimension, the force is smooth along the spatial dimension. Therefore, it may be possible to represent the control signal using a reduced set of basis (e.g., the Fourier basis), rather than with a different value for each indi-

<sup>‡</sup>There are 50 revolute joints (z rotation) and 50 universal joints (x and y rotations) for a total of 100 joints.

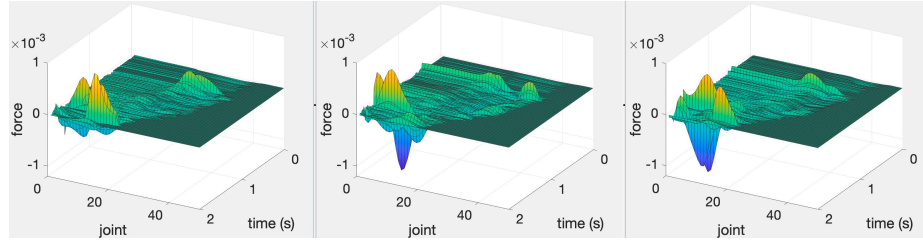


Fig. 8: Sliding force in inverse dynamics in x-axis, y-axis, and z-axis, respectively.

vidual segment. This may be an important clue for how a real hagfish controls its muscles while sliding the knot.

## 5 Conclusion

We presented a simulation technique for modeling a knotting hagfish. The simulator uses real-world biometric data that were collected from hands-on experiments. Our most significant contribution is our successful implementation of *positive thigmotaxis* using newly devised contact-based inverse dynamics. This allowed our hagfish model to slide the knot along the length of its body, which had not been successfully achieved using existing approaches. We hope that our work will enable researchers to characterize how hagfish control their bodies and to further develop better simulators that are biologically informative. Although the focus of this paper is on biological simulation, the positive thigmotaxis constraint may also be applicable to soft-robotics applications [30,36,28].

There are several features we would like to develop as future work. First, our current framework uses torques directly, rather than using muscle fibers. Adding contractile muscle fibers and computing the required activations would be an important next step toward a more biologically accurate simulator. We suspect that these activations can be represented by a reduced basis, as was the case with our torque-based simulation. Also, it would be interesting to model the deformable flesh with continuum mechanics, which would enable us to generate more accurate contact geometry. Next, we have only tried plain overhand knots for simplicity. It would be an interesting challenge to formulate other, more complicated knots that have been observed in nature. Lastly, the initial controller based on forward dynamics is hand crafted by trial and error. If we can obtain biologically correct muscular control signals, we would be able to generate much more realistic motions.

## Acknowledgements

We thank Austin Haney for helping to record video of knotting Pacific hagfish, *Eptatretus stoutii* and Washington Department of Fish and Wildlife officer

Donna Downs for their procurement. This work was supported in part by the National Science Foundation (IOS-1354788 to T.A.U. and CAREER-1846368 to S.S.).

## References

1. Adam, H.: Different types of body movement in the hagfish, *myxine glutinosa* l. *Nature* **188**(4750), 595–596 (1960)
2. Alexander, J.W., Briggs, G.B.: On types of knotted curves. *Annals of Mathematics* **28**(1/4), 562–586 (1926)
3. Andrew, W., Hickman, C.P.: *Histology of the vertebrates: a comparative text*. Mosby, Saint Louis (1974)
4. Baraff, D.: Fast contact force computation for nonpenetrating rigid bodies. In: *Proceedings of the 21st Annual Conference on Computer Graphics and Interactive Techniques*. pp. 23–34. SIGGRAPH '94, ACM, New York, NY, USA (1994)
5. Baumgarte, J.: Stabilization of constraints and integrals of motion in dynamical systems. *Comput. Methods in Appl. Mech. Eng.* **1**, 1–16 (Jun 1972)
6. Bergou, M., Wardetzky, M., Robinson, S., Audoly, B., Grinspun, E.: Discrete elastic rods. *ACM Trans. Graph.* **27**(3), 63:1–63:12 (Aug 2008)
7. Bertails, F., Audoly, B., Cani, M.P., Querleux, B., Leroy, F., L  v  que, J.L.: Super-helices for predicting the dynamics of natural hair. *ACM Trans. Graph.* **25**(3), 1180–1187 (Jul 2006)
8. Boyd, S., Vandenberghe, L.: *Convex Optimization*. Cambridge University Press (2004)
9. Brown, J., Latombe, J.C., Montgomery, K.: Real-time knot-tying simulation. *Vis. Comput.* **20**(2), 165–179 (May 2004)
10. Clark, A.J., Crawford, C.H., King, B.D., Demas, A.M., Uyeno, T.A.: Material properties of hagfish skin, with insights into knotting behaviors. *The Biological Bulletin* **230**(3), 243–256 (2016)
11. Clark, A.J., Summers, A.: Ontogenetic scaling of the morphology and biomechanics of the feeding apparatus in the Pacific hagfish *Eptatretus stoutii*, vol. 80. *Journal of Fish Biology* (2012)
12. Clubb, B.L., Clark, A.J., Uyeno, T.A.: Powering the hagfish “bite”: the functional morphology of the retractor complex of two hagfish feeding apparatuses. *Journal of morphology* **280**(6), 827–840 (2019)
13. Deul, C., Kugelstadt, T., Weiler, M., Bender, J.: Direct position-based solver for stiff rods. *Computer Graphics Forum* **37**(6), 313–324 (2018)
14. Evans, E., Hwang, Y., Sueda, S., Uyeno, T.A.: Estimating whole body flexibility in pacific hagfish. In: *The Society for Integrative & Comparative Biology* (January 3-7 2018)
15. Featherstone, R.: The calculation of robot dynamics using articulated-body inertias. *INT J ROBOT RES* **2**(1), 13–30 (1983)
16. Haney, W.A.: *Characterization of Body Knotting Behavior in Hagfish*. Master’s thesis, Valdosta State University (May 2017)
17. Jain, S., Liu, C.K.: Controlling physics-based characters using soft contacts. *ACM Trans. Graph.* **30**(6), 163:1–163:10 (Dec 2011)
18. Kaufman, D.M., Sueda, S., James, D.L., Pai, D.K.: Staggered projections for frictional contact in multibody systems. *ACM Trans. Graph.* **27**(5), 164:1–164:11 (Dec 2008)

19. Kim, J., Pollard, N.S.: Fast simulation of skeleton-driven deformable body characters. *ACM Trans. Graph.* **30**(5), 1–19 (2011)
20. Lee, Y., Park, M.S., Kwon, T., Lee, J.: Locomotion control for many-muscle humanoids. *ACM Trans. Graph.* **33**(6), 218:1–218:11 (Nov 2014)
21. Liu, L., Yin, K., Wang, B., Guo, B.: Simulation and control of skeleton-driven soft body characters. *ACM Trans. Graph.* **32**(6), 1–8 (2013)
22. Long, J.H., Koob-Emunds, M., Sinwell, B., Koob, T.J.: The notochord of hagfish *myxine glutinosa*: visco-elastic properties and mechanical functions during steady swimming. *Journal of Experimental Biology* **205**(24), 3819–3831 (2002)
23. Martini, F.H.: *The Ecology of Hagfishes*, pp. 57–77. Springer Netherlands (1998)
24. Miller, T.J.: Feeding behavior of *echidna nebulosa*, *enchelycore pardalis*, and *gymnomuraena zebra* (teleostei: Muraenidae). *Copeia* pp. 662–672 (1989)
25. Pai, D.K.: Strands: Interactive simulation of thin solids using cosserat models. *Computer Graphics Forum* **21**(3), 347–352 (2002)
26. Phillips, J., Ladd, A., Kavraki, L.E.: Simulated knot tying. In: *IEEE Int. Conf. Robot. Autom.* vol. 1, pp. 841–846. IEEE (2002)
27. Pickwell, G.V.: Knotting and coiling behavior in the pelagic sea snake *pelamis platurus* (l.). *Copeia* **1971**(2), 348–350 (1971)
28. Rus, D., Tolley, M.T.: Design, fabrication and control of soft robots. *Nature* **521**(7553), 467 (2015)
29. Shinar, T., Schroeder, C., Fedkiw, R.: Two-way coupling of rigid and deformable bodies. In: *Proc. SCA 2008*. pp. 95–103 (2008)
30. Simaan, N.: Snake-like units using flexible backbones and actuation redundancy for enhanced miniaturization. In: *Proc. ICRA 2005*. pp. 3012–3017 (April 2005)
31. Strahan, R.: The behaviour of myxinoids. *Acta Zoologica* **44**(1-2), 73–102 (1963)
32. Sueda, S., Jones, G.L., Levin, D.I.W., Pai, D.K.: Large-scale dynamic simulation of highly constrained strands. *ACM Trans. Graph.* **30**(4), 39:1–39:10 (Jul 2011)
33. Sueda, S., Kaufman, A., Pai, D.K.: Musculotendon simulation for hand animation. *ACM Trans. Graph.* **27**(3), 83:1–83:8 (Aug 2008)
34. Sumbre, G., Fiorito, G., Flash, T., Hochner, B.: Octopuses use a human-like strategy to control precise point-to-point arm movements. *Current biology : CB* **16**, 767–72 (05 2006)
35. Thelen, D.G., Anderson, F.C.: Using computed muscle control to generate forward dynamic simulations of human walking from experimental data. *Journal of biomechanics* **39**(6), 1107–1115 (2006)
36. Trivedi, D., Rahn, C.D., Kier, W.M., Walker, I.D.: Soft robotics: Biological inspiration, state of the art, and future research. *Applied Bionics and Biomechanics* **5**(3), 99–117 (2008)
37. Uyeno, T.A., Clark, A.J.: Muscle articulations: flexible jaw joints made of soft tissues. *Integrative and comparative biology* **55**(2), 193–204 (2015)
38. Vladu, I., Strîmbeanu, D., Ivănescu, M., Bizdoacă, N., Vladu, C., Florescu, M.: Control system for a hyper-redundant robot. *IFAC Proceedings Volumes* **45**(6), 853–858 (2012)
39. Wang, Y., Weidner, N.J., Baxter, M.A., Hwang, Y., Kaufman, D.M., Sueda, S.: REDMAX: Efficient & flexible approach for articulated dynamics. *ACM Transactions on Graphics* **38**(4), 104:1–104:10 (July 2019)
40. Zintzen, V., Roberts, C.D., Anderson, M.J., Stewart, A.L., Struthers, C.D., Harvey, E.S.: Hagfish predatory behaviour and slime defence mechanism. *Scientific Reports* **1**, 131 (2011)